

Article

Not peer-reviewed version

Integrated Metabolomics and Targeted Gene Expression Profiling Reveal the Arginine-Anthocyanin Axis in Pomegranate Aril Paleness Disorder

[Mehdi Rezaei](#)*, [Parviz Heidari](#), [Stefanie Reim](#)

Posted Date: 3 February 2026

doi: 10.20944/preprints202602.0233.v1

Keywords: aril; pomegranate metabolome; arginine–anthocyanin interaction; paleness disorder; integrative omics



Preprints.org is a free multidisciplinary platform providing preprint service that is dedicated to making early versions of research outputs permanently available and citable. Preprints posted at Preprints.org appear in Web of Science, Crossref, Google Scholar, Scilit, Europe PMC.

Copyright: This open access article is published under a [Creative Commons CC BY 4.0 license](#), which permit the free download, distribution, and reuse, provided that the author and preprint are cited in any reuse.

Disclaimer/Publisher's Note: The statements, opinions, and data contained in all publications are solely those of the individual author(s) and contributor(s) and not of MDPI and/or the editor(s). MDPI and/or the editor(s) disclaim responsibility for any injury to people or property resulting from any ideas, methods, instructions, or products referred to in the content.

Article

Integrated Metabolomics and Targeted Gene Expression Profiling Reveal the Arginine-Anthocyanin Axis in Pomegranate Aril Paleness Disorder

Mehdi Rezaei ^{1,2,*}, Parviz Heidari ³ and Stefanie Reim ⁴

¹ Horticultural Department, Agriculture Faculty, Shahrood University of Technology, Shahrood, Iran

² Center for International Scientific Studies & Collaboration (CISSC), Ministry of Science, Research and Technology of Iran

³ Department of Agronomy and Plant Breeding, Agriculture Faculty, Shahrood University of Technology, Shahrood, Iran

⁴ Julius Kühn-Institut (JKI), Federal Research Centre for Cultivated Plants, Institute for Breeding Research on Fruit Crops, Dresden-Pillnitz, Pillnitzer Platz 3a, 01326 Dresden, Germany

* Correspondence: Mhrezaei@shahroodut.ac.ir; Tel.: +98 233 239 2204

Abstract

Aril paleness (AP) is a new physiological disorder of pomegranate (*Punica granatum* L.) characterized by pale, dry and tasteless arils, while the peel remains healthy-looking. Its molecular basis is unknown. We used an integrated metabolomic and targeted gene expression approach on arils from four Iranian cultivars displaying no to severe AP symptoms. LC-MS profiling detected 617 reliable metabolites, with 266 metabolites consistently reduced in all symptomatic samples. Enrichment analysis revealed that arginine biosynthesis, glutathione metabolism and primary amino acid metabolism were the processes most strongly affected by AP. Protein interaction network analysis indicated that the arginine degradation pathway is the primary down-regulated module that interacts with the anthocyanin biosynthetic machinery, primarily through phenylalanine ammonia-lyase (PAL) hubs. Based on this network, seven genes representing both pathways were selected for targeted expression analysis. The qPCR analysis showed strong repression of *arginase* (*PgADS*, XM-031537872), *aldehyde dehydrogenase* (*PgAL12A1*, XM-031551051) and anthocyanin synthase (*PgOCHKF*, KF841619.1) in the cultivar 'Taroud' exhibiting severe AP symptoms compared with the symptom-free cultivar 'Damavand'. In contrast, phenylalanine ammonia-lyase (*PgPAL1*, KY094504.2) was unexpectedly induced 33-fold in the cultivar 'Taroud', while the downstream anthocyanin-related UDP-glucosyltransferase (*PgUGT*, MK058491.1) remained unchanged. These findings suggest that the collapse of arginine metabolism, combined with the downstream blockage of anthocyanin biosynthesis, underlie AP. These findings provide the first molecular insights into the mechanisms underlying AP, offering a basis for breeding and post-harvest strategies aimed at enhancing pomegranate's AP tolerance.

Keywords: aril; pomegranate metabolome; arginine–anthocyanin interaction; paleness disorder; integrative omics

Introduction

The pomegranate (*Punica granatum* L.) is a commercially significant fruit crop cultivated in subtropical and temperate regions with mild winters [1]. Global interest in this fruit has surged due to its high concentration of bioactive compounds, particularly its potent antioxidant properties [2,3]. Complementing its nutritional value, the pomegranate tree demonstrates considerable resilience to drought and low-fertility soils, facilitating its cultivation in arid areas across numerous countries,

including Iran, Turkey, India, Spain, and the United States [2]. In Iran, production is predominantly concentrated in the arid marginal areas of desert regions.

In recent decades, concurrent with global climate change, the incidence of physiological disorders in pomegranate, such as fruit cracking and sunburn, has increased markedly [1]. Among these, a novel disorder designated as "Aril Paleness" (AP) has emerged as a pervasive issue in most Iranian pomegranate orchards, severely compromising fruit marketability [4]. Fruits affected by AP, despite possessing a healthy external appearance, exhibit severely degraded internal aril quality—characterized by pale pigmentation, mealy and dehydrated texture, and an undesirable flavor, rendering them unsuitable for fresh consumption or processing [4,5]. When severity exceeds 50%, the fruit becomes entirely unmarketable. Field reports indicate that AP was first observed in 2006-2007 in the South Khorasan, Razavi Khorasan, and Semnan provinces of Iran, and was later reported in Yazd province as "baked pomegranates" [6]. It is now widespread across Iran and has also been reported in other pomegranate production areas, for example in the 'Ganesh' and 'Bhagwa' cultivars in India [7]. The AP pomegranates erode consumer confidence and create substantial challenges for export markets. Conventional horticultural interventions, including balanced mineral nutrition (Fe, Zn, K), shade netting, and post-harvest treatments, have provided only partial and inconsistent relief [8–10]. This erratic efficacy suggests that AP is not a simple nutrient deficiency but rather a systemic metabolic dysregulation whose underlying triggers remain obscure. Therefore, understanding AP requires moving beyond classical approaches to systems-level phenotyping.

The visual and internal quality of AP pomegranate fruit, including aril color, is directly dictated by its metabolic composition. The red color in pomegranate fruits is primarily attributed to the accumulation of anthocyanins, a prominent subclass of flavonoids [11]. Detailed metabolomic studies have revealed that pomegranate juice contains a wide variety of metabolites, including sugars, organic acids and amino acids. Most notably, it contains phenolic compounds [11,12]. Qin, *et al.* [13] reported 535 metabolites in the inner and outer peels, finding that monolignins were significantly accumulated in the inner seed coat layers. Zhao, Qi, Li, Cao, Liu, Yu, Xu and Qin [12] identified 23 flavones, 26 flavonoids, 15 flavanones, 11 catechins and their derivatives, 10 anthocyanins, and 4 proanthocyanidins. The accumulation of these compounds directly influences not only color but also flavor and the fruit's health-promoting properties.

Metabolomics, the comprehensive study of small molecules in a biological system, provides a snapshot of physiological status as influenced by genetics and environment [14]. This approach has proven powerful for dissecting color disorders in crops like beet root and sweet potato, revealing metabolic signatures that precede visible symptoms [15,16]. Environmental stresses can disrupt metabolic homeostasis, alter enzyme activity, and divert metabolic pathways. Conversely, transcriptomics, which involves analyzing genome-wide expression patterns, offers deep insights into the molecular mechanisms regulating these pathways. The integration of these two approaches is particularly powerful for pinpointing critical metabolites and their regulatory genes in response to stressors [16]. Despite recent advances in pomegranate physiology, a comprehensive study on AP using this integrated metabolomic and targeted gene expression has not been conducted.

Given this critical knowledge gap, we hypothesized that AP in pomegranate results from a specific reprogramming of primary and secondary metabolism. To test this, we combined untargeted LC-MS metabolomics with targeted qPCR analysis of key structural and regulatory genes in the arils of four Iranian pomegranate cultivars exhibiting a gradient of AP susceptibility. The objectives were to: (i) quantify metabolite changes associated with the disorder, (ii) identify the affected metabolic pathways, and (iii) validate the involvement of candidate genes linked to the observed pigment biosynthesis deficits. This research provides first molecular insights into AP and aims to identify biochemical markers that can support early detection and provide information for breeding of AP-tolerant pomegranate cultivars.

Materials and Methods

Plant Materials

Pomegranate fruits were harvested at commercial maturity from two climatically contrasting orchards in Shahroud county, Iran: a milder region (Mayami: 36.2433° N, 55.3910° E) and a warmer region (Torud: 36.4259° N, 55.0139° E). Arils were visually classified into four paleness categories according to symptom severity: no symptoms, slight, moderate, and severe. The four cultivars used were 'Damavand' (DN, no symptoms), 'Kashmar' (KN, slight; KW, moderate), and 'Torud' (TW, severe). DN, KN and KW fruit were picked in Mayami; TW fruits came from Torud, Shahroud, Iran. For each category, 12–25 fruits were randomly collected from each of three trees, constituting four independent biological replicates. For metabolomic analysis, arils were manually separated within two hours of harvest. The juice was immediately extracted using a stainless-steel laboratory press, clarified by filtration through two layers of cheesecloth, and approximately 15 mL per replicate was transferred to pre-weighed glass Petri dishes. The samples were covered with perforated Parafilm®, shell-frozen at -80°C , and subsequently lyophilized for 48 hours using a Vacuumer Freeze-Dryer (LTG Co., Germany). The resulting lyophilized powder was sealed and stored at -20°C in a desiccator containing silica gel until LC-MS analysis. For transcript analysis, 20 g of intact arils from each biological replicate were snap-frozen in liquid nitrogen and stored at -80°C for subsequent RNA extraction.

FTIR Analysis

Fourier-Transform Infrared (FTIR) spectroscopy was employed to analyze the chemical composition of pomegranate juice. This technique enables the identification of functional groups and investigation of molecular structure based on characteristic absorption patterns in the infrared region. FTIR spectra of juice samples from different pomegranate cultivars were obtained using an FTIR spectrometer (PerkinElmer, USA) covering the wavenumber range of 400 to 4000 cm^{-1} [17].

Metabolite Analysis

Metabolite profiling of pomegranate juice samples was performed following the methodology described by Qin, Liu, Li, Qi, Gao, Zhang, Yi, Pan, Ming and Xu [13]. Initially, 1g of freeze-dried sample was reconstituted with distilled water. The extracts were then analyzed using a Shimadzu UFLC system coupled to an AB Sciex 3200 mass spectrometer, equipped with a Kromasil 100-5 C18 column (150 mm \times 4.6 mm). The analysis employed a flow rate of 0.25 ml/min, a column temperature of 35°C, and an injection volume of 5 μL . The mobile phase consisted of solvent A (methanol with 0.1% formic acid) and solvent B (water with 0.1% formic acid). The gradient elution program for A:B (v:v) was set as follows: 10:90 at 0 min, 15:85 at 2 min, 50:50 at 12 min, 95:5 at 16 min, maintained at 95:5 until 50 min, and returned to 10:90 at 56 min. Following HPLC separation, mass spectrometric analysis was conducted using an LCMS API 6500 Q TRAP system equipped with a linear ion trap (LIT) and triple quadrupole (QQQ) mass analyzer. Detection was performed via electrospray ionization (ESI) in both positive and negative ion modes, controlled by Analyst 1.6.3 software (AB Sciex, Waltham). The optimized operational parameters were as follows: ESI source temperature, 475 $^{\circ}\text{C}$; nitrogen (grade 5) as the source gas; ion spray voltage floating (ISVF), 4.5 kV; declustering potential (DP), 70 V; and both GS1 and GS2 set to 40. The MZmine software (version 4.4) was used for processing the mass spectrometric data from all samples, including peak integration and chromatographic alignment [18]. The mass spectral peaks of identical metabolites across different samples were aligned to correct for retention time shifts. Metabolites were qualitatively and quantitatively analyzed according to the method described by Wang, Li, Ren, Gao, Zhang, Ma, Ma and Luo [15]. Compound identification was performed by matching MS data against public databases, primarily KNApSack [19], and by cross-referencing known pomegranate metabolites documented in the literature [12,20].

To identify differentially abundant metabolites, KN, KW, and TW cultivars were compared with DN (the symptom-free control) using a combined criterion of a Variable Importance in Projection (VIP) score ≥ 1 from multivariate analysis and a $|\text{Log}_2(\text{Fold Change})| \geq 1.5$ from univariate analysis. Metabolites meeting these criteria were subsequently submitted to MetaboAnalyst v.6.0 [21]. Significantly enriched metabolic and biosynthetic pathways associated with the metabolite list were identified using a False Discovery Rate (FDR) threshold of < 0.05 [22]. Furthermore, Venn diagrams illustrating the numbers of increased and decreased metabolites in the KN, KW, and TW sample groups were generated using the TBtools software [23].

Bioinformatics Analysis

An integrated bioinformatics approach was employed to investigate the molecular basis of AP. First, differentially abundant metabolites were identified based on the overlaps among the cultivars, as visualized by the Venn diagrams. These key metabolites were then subsequently subjected to pathway enrichment analysis using the Plant Metabolic Network (PMN) database [24]. This revealed a significant downregulation in several core metabolic pathways, most notably Arginine Biosynthesis, Tryptophan Metabolism, and Phenylalanine Metabolism. To contextualize these findings in relation to the visual symptoms of the disorder, the anthocyanin biosynthetic pathway, specifically for cyanidin-3-glucoside, was also mapped.

To link these metabolic findings with genetic regulation, we used the corresponding *Arabidopsis thaliana* genes involved in these key pathways as a reference. The STRING database [25] was then used to examine these candidate genes for possible functional interactions with known genes associated with anthocyanin biosynthesis. Network analysis revealed that among the downregulated metabolic pathways, only the arginine biosynthesis pathway showed significant functional associations with the anthocyanin biosynthetic machinery. Within this interactive network, genes encoding Phenylalanine Ammonia-Lyase (PAL1-4) demonstrated the highest connectivity, suggesting their pivotal role in linking arginine metabolism with anthocyanin biosynthesis.

Primer Design

For qPCR analysis, primers were designed to target pomegranate orthologs of previously identified *A. thaliana* genes. The coding sequences of the *A. thaliana* genes were obtained from the NCBI database (Table S-1) and used to perform BLASTp searches against the pomegranate proteome to find putative orthologs. Based on the aligned, conserved regions of these identified orthologs, specific primers were designed using Primer3 software (Table S-2).

Gene Expression Analysis

Total RNA was extracted from pomegranate aril tissues of both affected and healthy samples, with three biological replicates, using a modified hot phenol method [26]. The extracted RNA was treated with DNase I to remove genomic DNA contamination, and its concentration and purity were verified using a NanoDrop spectrophotometer (Termo Co. ND.ONE). cDNA was subsequently synthesized via cDNA Synthesis Kit (Parstous Co., Iran), and the resulting cDNA concentrations were normalized across all samples. Gene expression analysis was performed using quantitative real-time PCR (qPCR) with SYBR Green chemistry on a StepOne Plus™ system, employing gene-specific primers (Table S-2). The qPCR protocol consisted of an initial denaturation at 95°C for 5 minutes, followed by 40 cycles of denaturation at 95°C for 15 seconds and annealing/extension at 60°C for 45 seconds, with a subsequent melt curve analysis to confirm amplification specificity. Relative gene expression levels were calculated using the $2^{-\Delta\Delta C_t}$ method [27], and statistical significance between affected and control groups, DN, was determined using a Student's t-test.

Results and Discussion

FTIR Spectral Analysis

Fourier-Transform Infrared (FTIR) analysis of pomegranate juice samples revealed distinct spectral profiles correlating with AP severity (Figure 1). The spectra from healthy or only slightly affected samples (DN, KN) consistently showed more intense absorption in key functional group regions compared to affected samples (KW, TW). Notably, the broad O-H stretching band (3200-3400 cm^{-1}), indicative of phenolic compounds and sugars, was significantly more pronounced in healthy arils, suggesting a higher antioxidant content. A similar reduction in intensity was observed in affected samples for the C=O stretching peak ($\sim 1600 \text{ cm}^{-1}$), associated with carbonyl groups in organic acids and flavonoids, and the C-O stretching region ($\sim 1200 \text{ cm}^{-1}$), characteristic of carbohydrates and phenolics. Furthermore, spectral alterations in the 1000 cm^{-1} range in disordered samples implied structural changes in complex secondary metabolites.

Comparative FTIR analysis revealed a distinct metabolic profile in the healthy DN cultivar compared to cultivars affected by AP, most notably the severely affected TW. The DN spectrum was characterized by significantly higher absorption in regions associated with key quality compounds, including an 8.5-unit difference at 1034 cm^{-1} (C-N/C-O bonds of amines and esters), more intense peaks at 2917 cm^{-1} (C-H of lipids/proteins) and 1731 cm^{-1} (C=O of carbonyls/esters from sugars and fruit acids), and overall greater absorption in the 1400-870 cm^{-1} fingerprint region. Conversely, the susceptible TW cultivar exhibited a contrasting signature with higher absorption at 3560 cm^{-1} and 3075 cm^{-1} (N-H/C-H stretches, suggesting altered nitrogen metabolism) and at 734 cm^{-1} (C-C bonds), collectively indicating that the healthy fruit possesses a richer complement of flavor and aroma-related compounds, while the metabolic disruption in AP involves both a depletion of these desirable compounds and a shift in nitrogenous components.

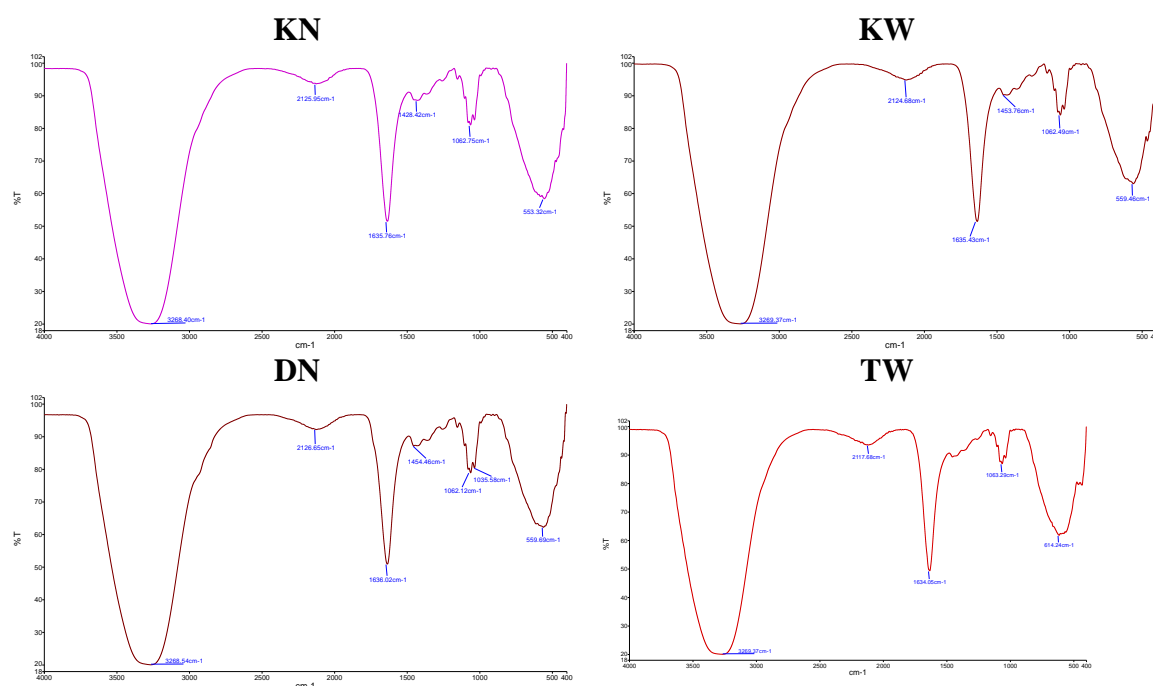


Figure 1. FTIR spectra of pomegranate juice from healthy and aril paleness-affected fruits. DN: healthy 'Damavand'; KN: 'Kashmar' (mild AP); KW: 'Kashmar' (severe AP); TW: 'Toroud' (severe AP).

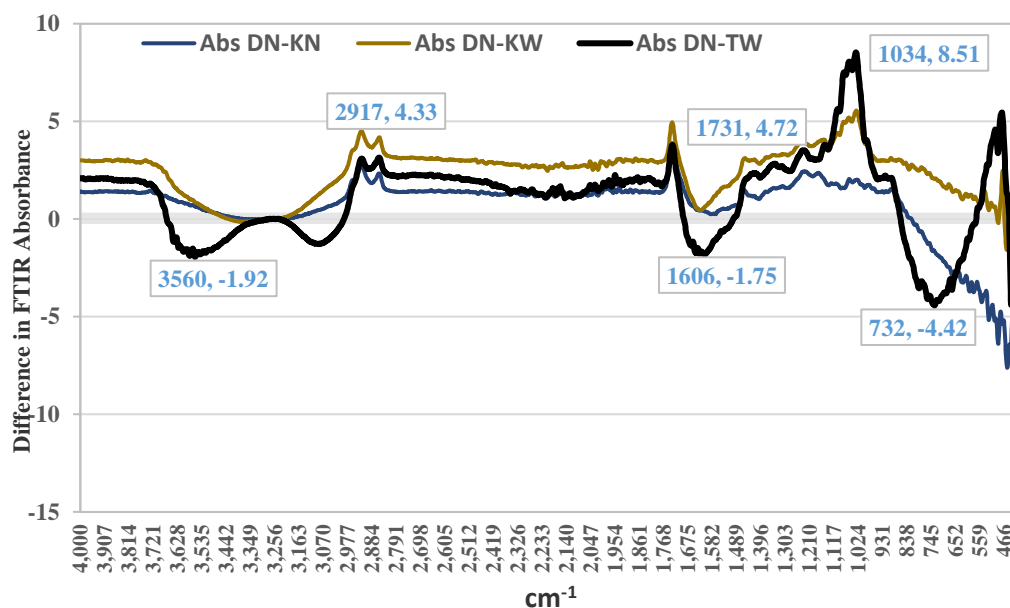


Figure 2. Absorbance differences in FTIR spectra between pomegranate cultivars affected by aril paleness disorder (TW, KN, KW) and a healthy cultivar (DN). DN: healthy 'Damavand'; KN: 'Kashmar' (mild AP); KW: 'Kashmar' (severe AP); TW: 'Toroud' (severe AP).

Metabolite Profiling

Comprehensive metabolite profiling of pomegranate cultivars revealed distinct chemical signatures associated with AP severity. A total of 1,198 metabolic features were detected across the four sample types, with m/z values spanning 51-999 Da. The chromatographic profiles showed cultivar-specific patterns, with the most intense peaks occurring at retention times of 8.9, 9.9, 9.5, and 2.5 minutes for DN, KN, KW, and TW samples, respectively. Mass spectral characteristics further distinguished the cultivars: while DN and KN samples showed predominant ions in the m/z 56-60 range, the severely affected TW cultivar exhibited its most abundant ion at m/z 453. Through targeted analysis, 617 metabolites (60-998 Da) were tentatively identified across all samples (Figure 3). Primary metabolites accounted for 151 compounds, including proteinogenic amino acids (glycine, alanine, valine, leucine), soluble sugars (glucose, fructose, sucrose), and organic acids (citric acid, malic acid). Secondary metabolites comprised 466 compounds, categorized as phenolic compounds (126), flavonoids and amines (150), terpenes (55), anthocyanins and derivatives (30), and other specialized metabolites (105). The comprehensive metabolite inventory provides a foundation for understanding the biochemical basis of AP disorder in pomegranate. Notable differences in metabolic abundance were observed among cultivars: DN (587 metabolites), TW (284), KN (135), and KW (174). The healthy DN cultivar showed the highest metabolic richness, containing key anthocyanins including cyanidin-3-glucoside, petunidin-3-arabinoside, and delphinidin-3-glucoside, along with other bioactive compounds such as quercetin, naringenin, and catechin that indirectly influence fruit coloration. The substantial metabolic disparity between healthy and affected cultivars underscores the profound impact of AP on the fruit's biochemical composition.

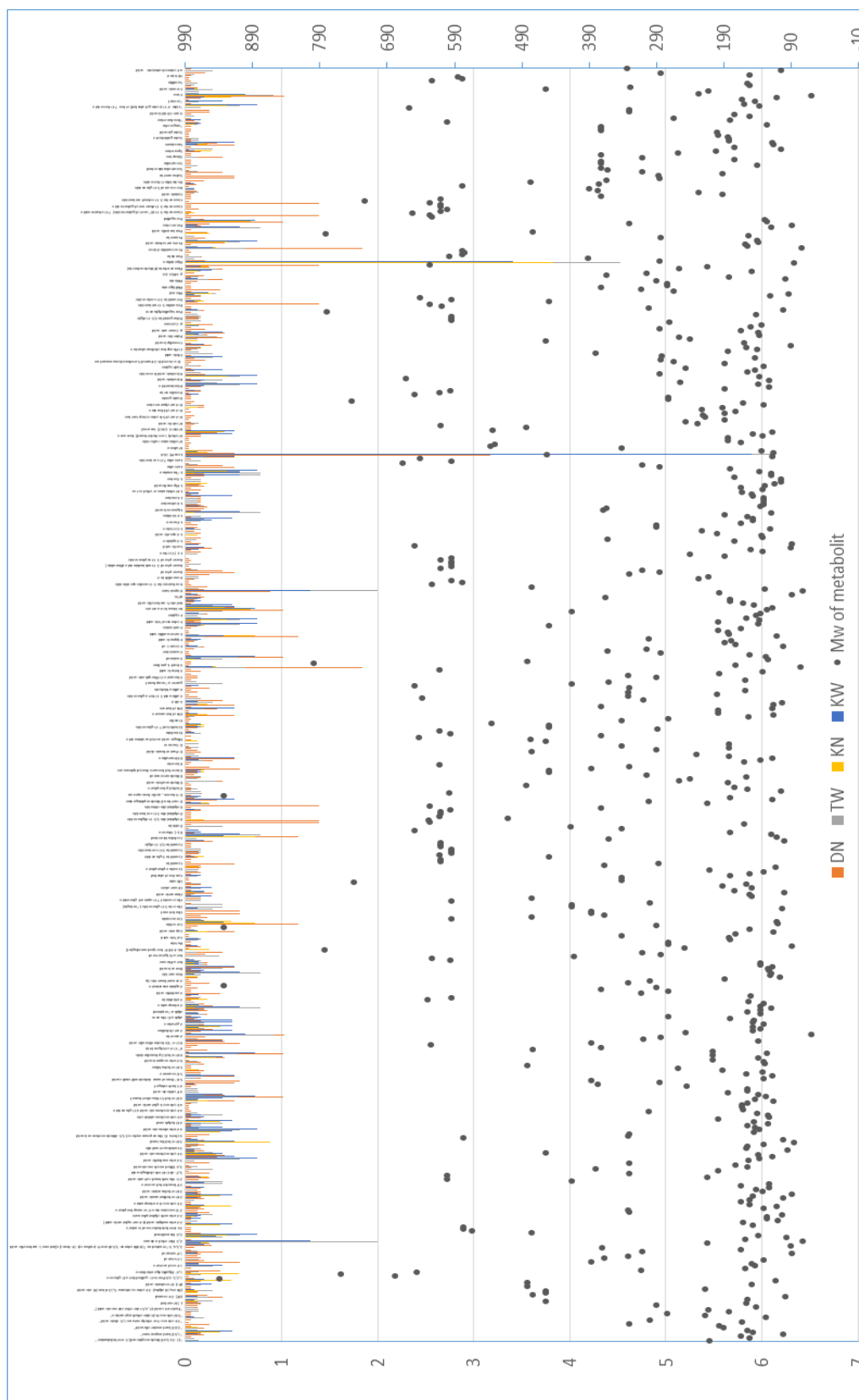


Figure 3. Metabolomic profiling and peak intensity in pomegranate juice affected by aril paleness disorder. DN: healthy 'Damavand'; KN: 'Kashmar' (mild AP); KW: 'Kashmar' (severe AP); TW: 'Toroud' (severe AP). Point : Molecular Weight (m/z), bar chart: peak intensity (cps).

Venn diagram analysis revealed distinct metabolic response patterns to AP disorder across pomegranate cultivars relative to healthy DN. The up-regulated metabolites demonstrated cultivar-

specific signatures, with KW, KN, and TW groups containing 16, 13, and 38 unique metabolites, respectively (Figure 4a). Notably, no metabolites were simultaneously upregulated in all three cultivars, suggesting the absence of a universal AP-induced metabolic response across genetic backgrounds. In contrast, down-regulated metabolites revealed a substantially different pattern (Figure 4b). A core set of 266 metabolites was consistently reduced across all affected cultivars, indicating a common disruption of fundamental metabolic processes underlying AP pathology. Beyond this shared response, each cultivar exhibited distinct metabolic reductions: KW (5 unique), KN (39 unique), and TW (11 unique). Additionally, 15 metabolites were co-down-regulated specifically between KW and TW cultivars, potentially reflecting severity-dependent metabolic repression (Figure 4b). These findings collectively indicate that AP disorder disrupts a conserved set of core metabolic pathways while simultaneously inducing cultivar-specific metabolic adjustments. The universally down-regulated metabolites likely represent the disorder's fundamental pathological footprint, whereas cultivar-unique metabolic profiles may reflect genetic variations in stress perception, adaptation mechanisms, or symptom severity.

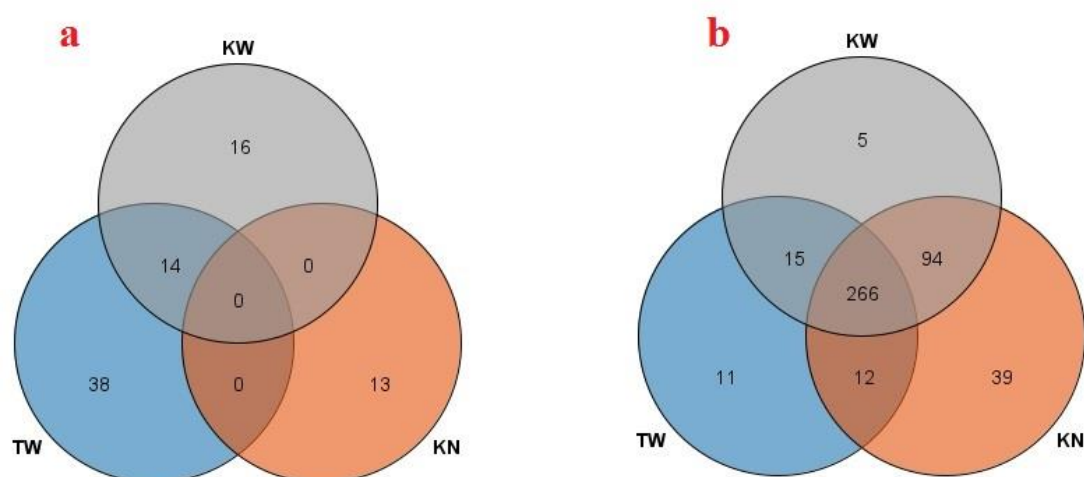


Figure 4. Venn diagrams showing differentially abundant metabolites in pomegranate juice cultivars affected by AP compared to the healthy DN cultivar. a: Up-regulated metabolites showing cultivar-specific increases. b: Down-regulated metabolites, with the large overlap (266 metabolites) indicating a common negative impact of the disorder. KW: 'Kashmar' (severe), KN: 'Kashmar' (mild), TW: 'Toroud' (severe). DN: 'Damavand' (healthy).

Pathway enrichment analysis of the 266 commonly downregulated metabolites across pomegranate cultivars with AP revealed significant disruptions in core metabolic pathways (Fig 5). The most severely affected was Arginine metabolism. This pathway is fundamental to nitrogen utilization and the synthesis of polyamines, which are critical for cell division and fruit development, processes likely impaired in AP disorder [28]. Concurrently, we observed a significant downregulation in Tryptophan metabolism and the linked Phenylalanine, Tyrosine, and Tryptophan biosynthesis pathway. This suppression suggests a major disruption in the biosynthesis of auxin, a key phytohormone governing fruit growth and morphology [29]. The downregulation of the Glutathione metabolism pathway indicates a compromised antioxidant system, which would make the aril cells highly vulnerable to oxidative damage, potentially contributing to the paleness and cellular degradation [30].

Furthermore, the disorder profoundly impacts energy metabolism. The reduced activity in the citrate cycle (TCA cycle) and starch and sucrose metabolism pathways points to a severe energy deficit and reduced carbon skeleton availability. In fruits, such a disruption directly compromises sugar accumulation and biomass production, leading to poor yield and quality [31]. Finally, alterations in biosynthesis of unsaturated fatty acids can destabilize cellular membrane integrity and

disrupt hormonal signaling, further exacerbating the physiological decline observed in AP-affected fruits [32].

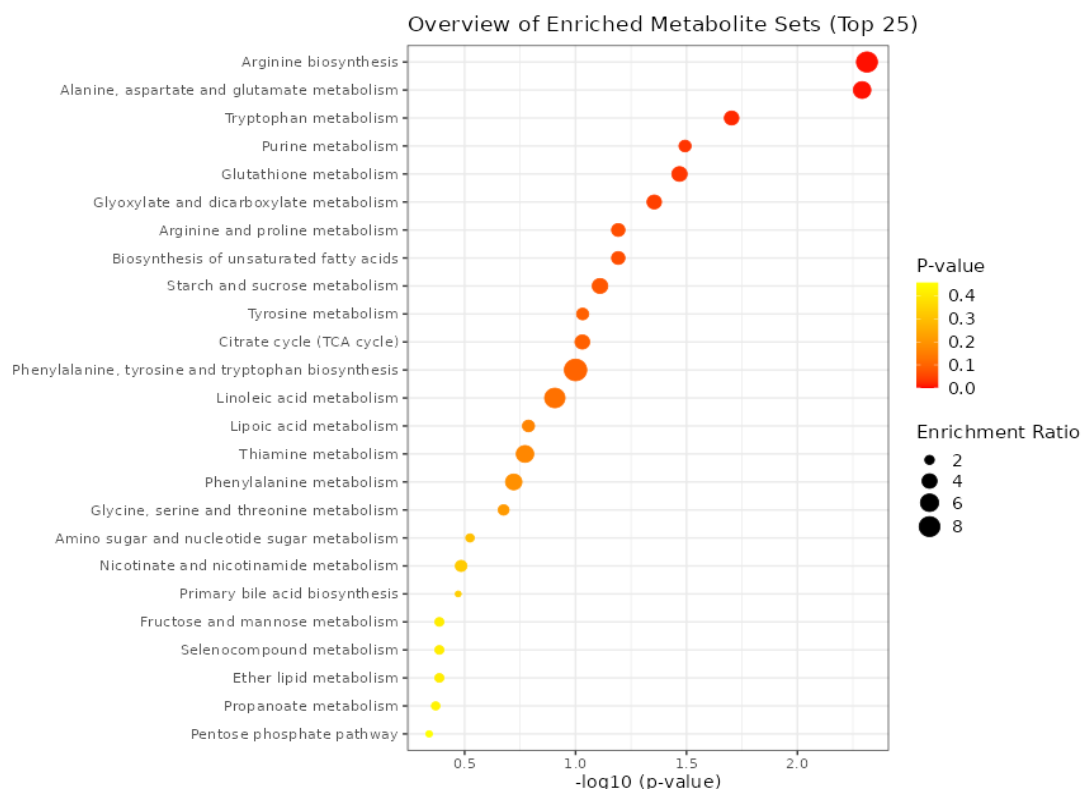


Figure 5. Pathway enrichment analysis of downregulated metabolites in pomegranate AP disorder. The bubble chart displays the top 25 significantly enriched metabolic pathways (FDR < 0.05) based on KEGG analysis. The x-axis represents the statistical significance ($-\log_{10}$ transformed p-value), bubble size indicates the enrichment ratio, and bubble color corresponds to the raw p-value.

Molecular Interaction Network Analysis

To elucidate the molecular mechanisms underlying color loss in AP disorder, we constructed a protein-protein interaction network integrating significantly downregulated metabolic pathways with the anthocyanin biosynthesis pathway from *A. thaliana*. Using the Plant Metabolic Network (PMN) and STRING databases, we aimed to identify key functional connections and nodal points between these systems. Among network analysis of tryptophan, aspartate, glutamate, and arginine metabolism with anthocyanin biosynthesis, the arginine degradation pathway demonstrated significant interactions with core anthocyanin biosynthesis components, primarily through shared nodes and intermediary pathways (Figure 6). Notably, phenylalanine ammonia-lyase genes (*PAL1-4*) emerged as the most highly connected nodes, forming multiple interactions with both arginine degradation and anthocyanin biosynthesis genes. To experimentally validate these bioinformatics predictions, we selected genes from the interconnected pathways - comprising seven arginine degradation genes, fourteen anthocyanin biosynthesis genes, and four phenylpropanoid-related genes (Table S1). Their homologs in the pomegranate genome were identified through BLAST analysis against NCBI databases. Six confirmed pomegranate genes were subsequently chosen for expression analysis in our experimental samples to directly investigate their involvement in AP disorder (Table S2).

the mildly affected KN cultivar, *PgAL12A1* expression increased relative to DN, suggesting an early compensatory mechanism aimed at maintaining glutamate availability despite the initial reduction in *PgAL12A1*. This upregulation likely supports the synthesis of protective metabolites during early stress. In contrast, *PgAL12A1* expression was reduced in the strongly affected KW cultivar. This decline is consistent with the dramatically reduced *PgADS* expression in KW, which severely limits the upstream metabolic flux into ornithine and glutamate. Under such conditions, the sustained supply of substrate for *PGAL12A1* diminishes, and cells under prolonged oxidative or metabolic stress often downregulate late-stage enzymatic steps. Thus, the reduction of *PGAL12A1* in KW likely reflects the exhaustion or failure of compensatory capacity under severe stress, rather than a regulatory response to increased arginine catabolism (which is, in fact, impaired).

The secondary decline in *PGAL12A1* expression in KW may therefore represent progressive metabolic collapse, driven by energy depletion, oxidative damage, or activation of programmed cell-death pathways. Together, these patterns point to a progressive breakdown of arginine catabolism as AP severity increases, contributing to nitrogen imbalance, reduced antioxidant capacity, and ultimately the manifestation of aril paleness.

Gene Expression Analysis of Genes in the Anthocyanin Pathway

Expression of both *PgOXXM*, XM_031520572, annotated as an oxygenase 2-oxoglutarate-dependent enzymes family and *PgOXXF*, KF841619.1, annotated as an anthocyanin synthase (ANS) gene was reduced in diseased arils. The reduction in *PgOXXF* expression was particularly evident in KW cultivar, whereas the reason for the increased expression detected in KN remains unclear. The family of 2-oxoglutarate-dependent enzymes (2-OGDs) plays a key role in anthocyanin biosynthesis [35]. Among them, *PgOXXF*, encoding ANS, is a key enzyme acting in the final steps of anthocyanin biosynthesis [36]. The strong downregulation of this gene in cultivars affected by AP is therefore consistent with impaired pigment accumulation. Previous studies on pomegranate have shown that the absence of ANS expression in cultivars with white arils is the main cause of lacking anthocyanin accumulation [36].

The transcript level of *PgUGT*, MK058491.1, was significantly increased in the TW cultivar with severe AP. In KN, expression was also increased compared to the healthy cultivar DN, although to a lesser degree. However, KW showed no significant differences in *PgUGT* expression compared to DN. UGT enzymes are involved not only in the glycosylation of anthocyanidins, but also in the modification of a wide range of substrates, including hormones, xenobiotics, and other secondary metabolites [37,38]. Increased expression *PgUGT* expression may therefore reflect a general response to oxidative stress or other cellular stresses occurring in AP-affected tissues. Under such conditions, the plants often enhance glycosylation to detoxify reactive compounds or restoring hormonal homeostasis. It is also possible that increased *PgUGT* expression leads to glycosylation of competing substrates (e.g. flavonols), reducing the availability of anthocyanidin for anthocyanin formation. Studies on *Freesia hybrida* have shown that different UGT isoforms can be functionally segregated and prefer different substrates (such as kaempferol versus quercetin and anthocyanidin) [37]. Thus, increased expression of a specific isoform (such as *PgUGT*) does not necessarily promote anthocyanin production and may even indirectly reduce pigment accumulation by diverting precursors into competing pathways (e.g flavonol production).

Expression of *PgPAL1*, KY094504.2, significantly increased (about 33-fold) in the TW cultivar which showed severe disease. In contrast, a decreasing trend was observed in other KN and KW. This contrasting pattern suggests a genotype-specific response to the AP and highlights the complexity of the underlying regulatory mechanisms. The pronounced induction of *PgPAL1* in TW may reflect a stronger defense response triggered by severe stress, leading to broad activation of the phenylpropanoid pathway. Seyed Hajizadeh, *et al.* [39] observed similar early PAL surge in rose petals supplied with arginine-loaded nano-chitosan, followed by anthocyanin decline once ethylene levels increased. PAL is the entry enzyme of the phenylpropanoid pathway, which not only provides

precursors for anthocyanins, but also generates numerous defense-related compounds such as phytoalexins, lignin (cell wall strengthening) and other antioxidant phenolics [40,41].

The reduced *PgPAL1* expression in KN and KW may indicate that these cultivars prioritize alternative defense pathways, such as the glutathione system or proline accumulation, over activation of the phenylpropanoid pathway. Differences in genetic background and environmental conditions may contribute to these cultivar-specific responses. Since TW was sampled in a warmer region (Torud) and showed more severe symptoms, these factors may have acted as stronger triggers for defense signaling and consequently for *PgPAL1* overexpression.

Finally, the expression of *PgADT1*, XM-031536172, encoding arogenate dehydratase involved in phenylalanine biosynthesis, was reduced in diseased samples compared to the healthy control. In *Arabidopsis*, the *ADT2* isoform is essential for seed growth and development [42]. *ADT* participates in both the arogenate and phenylpyruvate pathways leading to phenylalanine formation. Since phenylalanine is not only fundamental for protein synthesis but also the primary substrate for *PAL* in the phenylpropanoid pathway, reduced *PgADT1* expression may limit precursor availability for anthocyanin production [41]. This suggests that disruptions in upstream steps of aromatic amino acid biosynthesis may contribute to AP development in pomegranate.

The overall pattern of gene expression in this study suggests a coordinated disruption of the interconnected network of nitrogen metabolism and the anthocyanin biosynthesis pathway in AP arils. Reduced expression of key genes in the arginine degradation pathway (*PgADS* and *PgAL12A1*) suggests that nitrogen metabolism is not functioning properly in these tissues. This disruption is likely to increase oxidative stress by reducing the production of protective polyamines on the one hand, and to affect downstream pathways by disrupting amino acid balance on the other. Simultaneously, a severe reduction in the expression of key genes of the anthocyanin pathway, especially anthocyanin synthase (*PgOXXF*) and glycosyltransferase (*PgUGT*), clearly explains the lack of pigment in AP arils. The phenylalanine ammonia lyase gene (*PgPAL1*) appears as a connecting node between these two pathways. In summary, pomegranate AP appears to be a multifactorial phenomenon characterized at the molecular level by disruption of the nitrogen cycle (especially the arginine pathway) and blockage of the anthocyanin biosynthesis pathway at the final stages.

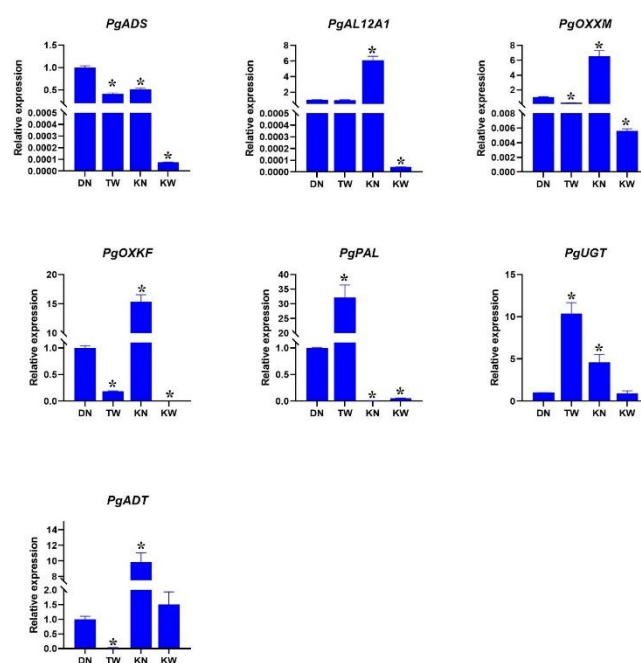


Figure 5. Relative expression patterns ($2^{-\Delta CT}$) of key genes involved in arginine metabolism and anthocyanin biosynthesis across pomegranate cultivars with varying susceptibility to AP. (A) Arginase (*PgARG*), (B) Aldehyde dehydrogenase (*PgALDH*), (C) Oxidase (*PgOXX*), (D) Anthocyanin synthase (*PgANS*), (E)

Phenylalanine ammonia-lyase (PgPAL), (F) Glycosyltransferase (PgUGT), and (G) Argonate dehydrogenase (PgADH). DN: Healthy 'Damavand' cultivar; KN: 'Kashmar' with mild symptoms; KW: 'Kashmar' with severe symptoms; TW: 'Toroud' with severe symptoms. Asterisks above bars indicate significant differences ($p < 0.05$, Student's t-test) compared to the healthy control (DN).

Conclusion

This work establishes the biochemical and molecular foundation for understanding AP disorder and demonstrates the power of integrative omics approaches in dissecting complex physiological disorders. The identification of the arginine-anthocyanin axis provides mechanistic insight and establishes the 266-metabolite signature as potential diagnostic markers for pre-symptomatic detection in breeding programs. While significant progress has been made, the precise environmental triggers and potential for metabolic engineering to enhance tolerance remain critical areas for future investigation. The cultivar-specific responses observed here underscore the importance of considering genetic background in both research and practical management of this economically significant disorder. These findings provide a solid basis for future studies to target manipulation of these pathways (such as exogenous application of precursors or gene expression regulators) to reduce the damage caused by this condition and provide actionable targets for developing AP-resistant cultivars and effective management strategies to ensure pomegranate fruit quality in a changing climate.

Supplementary Materials: The following supporting information can be downloaded at the website of this paper posted on Preprints.org.

Author Contributions: Conceptualization, M.R. and P.H. ; methodology, M.R., P.H. and E.R.; formal analysis, M.R. and P.H. ; investigation, M.R.; data curation, M.R. and P.H. ; writing— original draft preparation, M.R. ; writing—review and editing, M.R., P.H. and E.R.; project administration, M.R. ; funding acquisition, M.R. and P.H.; All authors have read and agreed to the published version of the manuscript.

Funding: This work was supported by the Center for International Scientific Studies & Collaboration (CISSC), Ministry of Science, Research and Technology of Iran.

Data Availability Statement: The data supporting the findings of this study are included in the article and supplementary materials. Further inquiries can be directed to the corresponding author.

Conflicts of Interest: The authors declare that they have no conflict of interest to report.

References

1. Yilmaz, C.; Rezaei, M.; Sarkhosh, A. *Environmental requirements and site selection*; CABI: 2021; pp. 225–246.
2. Sarkhosh, A.; Yavari, A.M.; Zamani, Z. *The pomegranate: Botany, production and uses*; CAB International: 2021.
3. Kalaycıoğlu, Z.; Erim, F.B. Total phenolic contents, antioxidant activities, and bioactive ingredients of juices from pomegranate cultivars worldwide. *Food Chemistry* **2017**, *221*, 496-507, doi:10.1016/j.foodchem.2016.10.084.
4. Tabar, S.M.; Tehranifar, A.; Davarynejad, G.H.; Nemati, S.H.; Zabihi, H.R. Aril paleness, new physiological disorder in pomegranate fruit (*Punica granatum*): physical and chemical changes during exposure of fruit disorder. **2009**.
5. Kavand, M.; Arzani, K.; Barzegar, M.; Mirlatifi, M.J.J.o.A.S.; Technology. Pomegranate (*Punica granatum* L.) fruit quality attributes in relation to aril browning disorder. **2020**, *22*, 1053-1065.
6. Kavand, M.; Arzani, K.; Barzegar, M.; Mirlatifi, M. Identification of the tolerant pomegranate genotypes for the aril browning or aril paleness disorder. In Proceedings of the I International Conference and X National Horticultural Science Congress of Iran (IrHC2017) 1315, 2017; pp. 609-614.
7. Shivashankar, S.; Hemlata, S.; Sumathi, M.J. Aril browning in pomegranate (*Punica granatum* L.) is caused by the seed. *Current Science* **2012**, *103*, 26-28.

8. Asadi, E.; Ghehsareh, A.M.; Moghadam, E.G.; Hodaji, M.; Zabihi, H. Improving of pomegranate aril paleness disorder through application of Fe and Zn elements. *Indian Journal of Horticulture* **2019**, *76*, 279-288.
9. Jahani, M.; Sayyari Zohan, M.; Moradinezhad, F.; Mirzaee, M.R.; Khayyat, M. Effectiveness of potassium spraying on mitigation of aril paleness disorder in different pomegranate cultivars. *Journal of Plant Nutrition* **2024**, *47*, 3024-3034.
10. Kavand, M.; Arzani, K.; Barzegar, M.; Mirlatifi, M.J.S.; Journal, P.P. Effects of sunscreen, kaolin application, fruit thinning and supplementary irrigation on the aril browning disorder of Pomegranate cv. "Malase Torshe Saveh". **2017**, *33*, 85-112.
11. Krueger, D.A. Composition of Pomegranate Juice. *Journal of AOAC INTERNATIONAL* **2019**, *95*, 163-168, doi:10.5740/jaoacint.11-178.
12. Zhao, J.; Qi, X.; Li, J.; Cao, Z.; Liu, X.; Yu, Q.; Xu, Y.; Qin, G. Metabolic Profiles of Pomegranate Juices during Fruit Development and the Redirection of Flavonoid Metabolism. *Horticulturae* **2023**, *9*, 881.
13. Qin, G.; Liu, C.; Li, J.; Qi, Y.; Gao, Z.; Zhang, X.; Yi, X.; Pan, H.; Ming, R.; Xu, Y. Diversity of metabolite accumulation patterns in inner and outer seed coats of pomegranate: exploring their relationship with genetic mechanisms of seed coat development. *Horticulture Research* **2020**, *7*.
14. Chele, K.H.; Tinte, M.M.; Piater, L.A.; Dubery, I.A.; Tugizimana, F. Soil salinity, a serious environmental issue and plant responses: A metabolomics perspective. *Metabolites* **2021**, *11*, 724.
15. Wang, A.; Li, R.; Ren, L.; Gao, X.; Zhang, Y.; Ma, Z.; Ma, D.; Luo, Y. A comparative metabolomics study of flavonoids in sweet potato with different flesh colors (*Ipomoea batatas* (L.) Lam). *Food Chemistry* **2018**, *260*, 124-134, doi:10.1016/j.foodchem.2018.03.125.
16. Liu, L.; Wang, B.; Liu, D.; Zou, C.; Wu, P.; Wang, Z.; Wang, Y.; Li, C.J.B.p.b. Transcriptomic and metabolomic analyses reveal mechanisms of adaptation to salinity in which carbon and nitrogen metabolism is altered in sugar beet roots. **2020**, *20*, 1-21.
17. Vardin, H.; Tay, A.; Ozen, B.; Mauer, L. Authentication of pomegranate juice concentrate using FTIR spectroscopy and chemometrics. *Food Chemistry* **2008**, *108*, 742-748, doi:10.1016/j.foodchem.2007.11.027.
18. Schmid, R.; Heuckeroth, S.; Korf, A.; Smirnov, A.; Myers, O.; Dyrland, T.S.; Bushuiev, R.; Murray, K.J.; Hoffmann, N.; Lu, M.; et al. Integrative analysis of multimodal mass spectrometry data in MZmine 3. *Nature Biotechnology* **2023**, *41*, 447-449, doi:10.1038/s41587-023-01690-2.
19. KNApSAcK. KNApSAcK Database (2024). KNApSAcK Metabolite Database. . **2024**.
20. Zhao, X.; Shen, Y.; Yan, M.; Yuan, Z. Flavonoid profiles in peels and arils of pomegranate cultivars. *Journal of Food Measurement and Characterization* **2022**, *16*, 880-890, doi:10.1007/s11694-021-01216-x.
21. Chong, J.; Xia, J. MetaboAnalystR: an R package for flexible and reproducible analysis of metabolomics data. *Bioinformatics* **2018**, *34*, 4313-4314, doi:10.1093/bioinformatics/bty528.
22. Benjamini, Y.; Hochberg, Y. Controlling the False Discovery Rate: A Practical and Powerful Approach to Multiple Testing. *Journal of the Royal Statistical Society: Series B (Methodological)* **2018**, *57*, 289-300, doi:10.1111/j.2517-6161.1995.tb02031.x.
23. Chen, C.; Chen, H.; Zhang, Y.; Thomas, H.R.; Frank, M.H.; He, Y.; Xia, R. TBtools: An Integrative Toolkit Developed for Interactive Analyses of Big Biological Data. *Molecular Plant* **2020**, *13*, 1194-1202, doi:10.1016/j.molp.2020.06.009.
24. Hawkins, C.; Xue, B.; Yasmin, F.; Wyatt, G.; Zerbe, P.; Rhee, Seung Y. Plant Metabolic Network 16: expansion of underrepresented plant groups and experimentally supported enzyme data. *Nucleic Acids Research* **2024**, *53*, D1606-D1613, doi:10.1093/nar/gkac991.
25. Szklarczyk, D.; Kirsch, R.; Koutrouli, M.; Nastou, K.; Mehryary, F.; Hachilif, R.; Gable, A.L.; Fang, T.; Doncheva, N.T.; Pyysalo, S.; et al. The STRING database in 2023: protein-protein association networks and functional enrichment analyses for any sequenced genome of interest. *Nucleic Acids Res* **2023**, *51*, D638-d646, doi:10.1093/nar/gkac1000.
26. Liu, L.; Han, R.; Yu, N.; Zhang, W.; Xing, L.; Xie, D.; Peng, D. A method for extracting high-quality total RNA from plant rich in polysaccharides and polyphenols using *Dendrobium huoshanense*. *PloS one* **2018**, *13*, e0196592.

27. Livak, K.J.; Schmittgen, T.D. Analysis of relative gene expression data using real-time quantitative PCR and the 2⁻ΔΔCT method. *methods* **2001**, *25*, 402-408.
28. Alcázar, R.; Altabella, T.; Marco, F.; Bortolotti, C.; Reymond, M.; Koncz, C.; Carrasco, P.; Tiburcio, A.F. Polyamines: molecules with regulatory functions in plant abiotic stress tolerance. *Planta* **2010**, *231*, 1237-1249, doi:10.1007/s00425-010-1130-0.
29. Zhao, Y. Auxin biosynthesis: a simple two-step pathway converts tryptophan to indole-3-acetic acid in plants. *Mol Plant* **2012**, *5*, 334-338, doi:10.1093/mp/ssr104.
30. Foyer, C.H.; Noctor, G. Ascorbate and glutathione: the heart of the redox hub. *Plant Physiol* **2011**, *155*, 2-18, doi:10.1104/pp.110.167569.
31. Carrari, F.; Fernie, A.R. Metabolic regulation underlying tomato fruit development. *J Exp Bot* **2006**, *57*, 1883-1897, doi:10.1093/jxb/erj020.
32. Upchurch, R.G. Fatty acid unsaturation, mobilization, and regulation in the response of plants to stress. *Biotechnol Lett* **2008**, *30*, 967-977, doi:10.1007/s10529-008-9639-z.
33. Lv, J.; Pang, Q.; Chen, X.; Li, T.; Fang, J.; Lin, S.; Jia, H. Transcriptome analysis of strawberry fruit in response to exogenous arginine. *Planta* **2020**, *252*, 82.
34. Hilbert, G.; Soyer, J.; Gaudillere, J.; Molot, C.; Giraudon, J. MilinS, Nitrogen supply during growth of *Vitis vinifera* L cv Merlot: effect on must quality and anthocyanin accumulation. *Vitis* **2003**, *42*, 69-76.
35. Wang, Y.; Shi, Y.; Li, K.; Yang, D.; Liu, N.; Zhang, L.; Zhao, L.; Zhang, X.; Liu, Y.; Gao, L.; et al. Roles of the 2-Oxoglutarate-Dependent Dioxygenase Superfamily in the Flavonoid Pathway: A Review of the Functional Diversity of F3H, FNS I, FLS, and LDOX/ANS. *Molecules* **2021**, *26*, 6745.
36. Zhao, X.; Yuan, Z.; Feng, L.; Fang, Y. Cloning and expression of anthocyanin biosynthetic genes in red and white pomegranate. *Journal of plant research* **2015**, *128*, 687-696.
37. Meng, X.; Li, Y.; Zhou, T.; Sun, W.; Shan, X.; Gao, X.; Wang, L. Functional Differentiation of Duplicated Flavonoid 3-O-Glycosyltransferases in the Flavonol and Anthocyanin Biosynthesis of *Freesia hybrida*. *Frontiers in Plant Science* **2019**, Volume 10 - 2019, doi:10.3389/fpls.2019.01330.
38. Kim, H.S.; Kim, B.-G.; Sung, S.; Kim, M.; Mok, H.; Chong, Y.; Ahn, J.-H. Engineering flavonoid glycosyltransferases for enhanced catalytic efficiency and extended sugar-donor selectivity. *Planta* **2013**, *238*, 683-693, doi:10.1007/s00425-013-1922-0.
39. Seyed Hajzadeh, H.; Rouhpourazar, M.; Azizi, S.; Zahedi, S.M.; Okatan, V. Nanochitosan-based encapsulation of arginine and phenylalanine improves the quality and vase life of *Rosa hybrida* 'Morden Fireglow'. *Journal of Plant Growth Regulation* **2024**, *43*, 686-700.
40. Ben-Simhon, Z.; Judeinstein, S.; Nadler-Hassar, T.; Trainin, T.; Bar-Ya'akov, I.; Borochoy-Neori, H.; Holland, D. A pomegranate (*Punica granatum* L.) WD40-repeat gene is a functional homologue of Arabidopsis TTG1 and is involved in the regulation of anthocyanin biosynthesis during pomegranate fruit development. *Planta* **2011**, *234*, 865-881, doi:10.1007/s00425-011-1438-4.
41. Perkowski, M.C.; Warpeha, K.M. Phenylalanine roles in the seed-to-seedling stage: Not just an amino acid. *Plant Science* **2019**, *289*, 110223.
42. El-Azaz, J.; Cánovas, F.M.; Ávila, C.; de la Torre, F. The Arogenate Dehydratase ADT2 is Essential for Seed Development in Arabidopsis. *Plant and Cell Physiology* **2018**, *59*, 2409-2420, doi:10.1093/pcp/pcy200.

Disclaimer/Publisher's Note: The statements, opinions and data contained in all publications are solely those of the individual author(s) and contributor(s) and not of MDPI and/or the editor(s). MDPI and/or the editor(s) disclaim responsibility for any injury to people or property resulting from any ideas, methods, instructions or products referred to in the content.